DSE--4042-1

CADMIUM SULFIDE - COPPER SULFIDE

HETEROJUNCTION CELL RESEARCH

PATENT CLEARED
BROOKHAVEN PATENT BRANCH

Quarterly Progress Report -1

September 1, 1978 - December 1, 1978

MASTER

XR-9-8063-1-01

June 1979

INSTITUTE OF ENERGY CONVERSION
UNIVERSITY OF DELAWARE
NEWARK, DELAWARE 19711

Supported by the Solar Energy Research Institute, Report XR-9-8063-1-01

DISTRIBUTION OF THIS DOCUMENT IS UNLIMITED

DISCLAIMER

This report was prepared as an account of work sponsored by an agency of the United States Government. Neither the United States Government nor any agency Thereof, nor any of their employees, makes any warranty, express or implied, or assumes any legal liability or responsibility for the accuracy, completeness, or usefulness of any information, apparatus, product, or process disclosed, or represents that its use would not infringe privately owned rights. Reference herein to any specific commercial product, process, or service by trade name, trademark, manufacturer, or otherwise does not necessarily constitute or imply its endorsement, recommendation, or favoring by the United States Government or any agency thereof. The views and opinions of authors expressed herein do not necessarily state or reflect those of the United States Government or any agency thereof.

DISCLAIMER

Portions of this document may be illegible in electronic image products. Images are produced from the best available original document.

CADMIUM SULFIDE - COPPER SULFIDE
HETEROJUNCTION CELL RESEARCH

Quarterly Progress Report

September 1, 1978 - December 1, 1978

XR-9-8063-1

June 1979

DISCLAIMER

This book was prepared as an account of work sponsored by an agency of the United States Government. Neither the United States Government nor any agency thereof, nor any of their employees, makes any warranty, express or implied, or assumes any legal liability or responsibility for the accuracy, completeness, or usefulness of any information, apparatus, product, or process disclosed, or represents that its use would not infringe privately owned rights. Reference herein to any specific commercial product, process, or service by trade name, trademark, manufacturer, or otherwise, does not necessarily constitute or imply its endorsement, recommendation, or favoring by the United States Government or any agency thereof. The views and opinions of authors expressed herein do not necessarily state or reflect those of the United States Government or any agency thereof.

INSTITUTE OF ENERGY CONVERSION
UNIVERSITY OF DELAWARE
NEWARK, DELAWARE 19711

Supported by the Solar Energy Research Institute, Report XR-9-8063-1-01

DISTRIBUTION OF THIS DOCUMENT IS UNLIMITED

1. ABSTRACT

The CdS/Cu_2S cell development effort has now shifted to the planar junction cell. It has been shown that this junction gives a higher open circuit voltage than that achieved with the highly textured cell structure. Optical measurements have shown that applying a two-layer anti-reflection coating to the planar cell does not achieve the high photon economy shown by the textured structure. Total reflectance measurements have revealed that this is due to the lack of light trapping in the planar structure. Modified cell designs are now being developed with the planar junction necessary for high open circuit voltage while achieving the necessary light trapping. Work on the $(CdZn)S/Cu_2S$ cell has revealed that cell performance is extremely sensitive to the method of Cu_2S production. Appropriate structural studies have been initiated to identify the underlying reasons. Theoretical analysis and modeling of the current flow in the Cu_2S layer has shown that the conventional one-dimensional analysis can lead to significant errors in interpreting the effects of sheet resistance. A rigorous two-dimensional current analysis is being conducted. The importance of the changes in absorption coefficient of the Cu_2S stoichiometry has been identified and the relation between stoichiometry, resistivity and absorption coefficient derived. On the basis of a review of the encapsulation task in the large scale silicon array program it has been determined that inorganic glasses are probably the only viable encapsulant for a CdS/Cu_2S cell.

2. TABLE OF CONTENTS

1. Abstract

2. Table of Contents

   List of Illustrations

   List of Tables

3. Introduction

4. Cell Production, Analysis Testing

   4.1 Development of CdS/Cu_2S Solar Cells

   4.2 Development of $(CdZn)S/Cu_2S$ Solar Cells

   4.3 Electro-Optical Analysis

   4.4 Encapsulation for Improved Stability

5. Future Developments

6. References

APPENDIX A - "Measurements of Interface Recombination Velocity by Capacitance/Collection Efficiency Variation in Cu_2S/CdS Heterojunctions by N. Convers Wyeth and A. Rothwarf.

LIST OF FIGURES

Figure 1 Influence of a Two Layer Anti-Reflection Coating on Total Reflectance. Theory and Experiment.

Figure 2 Total Reflectance Measurements for CdS/Cu_2S and $(CdZn)S/Cu_2S$ Solar Cells.

Figure 3 Time Dependent Decay of Open Circuit Voltage for $(CdZn)S/Cu_2S$ Cells Made in Various Ways.

Figure 4 Calculated Variation of Carrier Density, Resistivity and Normalized Absorption Coefficient as a Function of the Position of the Fermi Level.

Figure 5 Calculated and Experimental Values for Sheet Resistance and Absorption Coefficient in Cu_2S for $\lambda = 650$ nm. Data Points are taken from Reference 5 and Corrected for Absorption in CdS and Reflection Losses.

Figure 6 As for Fig. 5 at $\lambda = 750$ nm

Figure 7 As for Fig. 5 at $\lambda = 850$ nm

LIST OF TABLES

Table 1 Influence of Junction Formation on Open Circuit Voltage

Table 2 Comparison of $(CdZn)S/Cu_2S$ and CdS/Cu_2S Solar Cell Data

Table 3 Influence of Cu_2S Sheet Resistance on Computed Fill Factor According to Various Analyses

3. INTRODUCTION

Under the previous contract EG-77-C-03-1576 a broad-based research and development effort on thin film solar cells based on the CdS/Cu_2S junction has been carried out. The cell development efforts were divided into two cell development tasks on CdS/Cu_2S and $(CdZn)S/Cu_2S$. The third task consisted of theoretical modeling, and experimental and theoretical analysis to direct and drive the cell development efforts. The fourth task, at a limited level of effort, was aimed at improving the knowledge and understanding of the factors controlling long-term cell stability.

As a result of the previous effort a textured CdS/Cu_2S cell of 9.15% conversion efficiency had been developed. A total loss analysis of that cell indicated that further improvements in efficiency with that design would be very limited. Accordingly the present project is aimed at developing a substantially higher efficiency cell with a planar structure instead of the previous highly textured design.

The development of the mixed sulfide cell had progressed to the point where efficiencies of over 7% had been realized. A substantial effort had been devoted to developing a controlable and reproducible technique for depositing thin films of (CdZn)S with the electrical, optical and morphological properties determined to be necessary from the research on the CdS/Cu_2S cell.

The level of understanding of the operation of the CdS/Cu_2S heterojunction has continued to improve and a basically quantitative description has now been formulated. In order to determine the mechanisms taking place in any particular cell a range of specialized optical and electronic techniques have been developed and applied to the textured cell. Some effort has also been

devoted to applying the same type of analysis to the mixed sulfide cell, but at the end of the previous contract the understanding of this cell was considerably less complete than that for the traditional CdS/Cu_2S cell.

Experiments on the influence of thermal treatments and oxidation or reducing atmospheres on the behavior of the CdS/Cu_2S cell have served to identify the oxidation of the Cu_2S layer as the primary cause of most of the reported losses in cell performance. Previous modeling which suggested that the inter-diffusion of copper into the CdS layer would impose a limiting usable life on the cell have tended to be discounted by the more recent research. The previous model was that as copper diffuses into the CdS causing compensation the electric field at the junction will decline resulting in a loss in current collection. It has now been shown that, although a decrease in dark capacitance is observed with thermal treatment of the CdS/Cu_2S cell, this effect is overwhelmed in the light by the trapping of holes at centers in the CdS. The trapped charge restores the high fields at the junction, and in consequence good current collection is possible even in cells that have been subjected to very protracted heat treatments.

During the first quarter of the present program the work on planar junction CdS/Cu_2S cells has shown that the anticipated higher open circuit voltages can be achieved. The initial assumption that a simple two layer anti-reflection coating on the front surface of the cell would give adequate photon economy has been shown to be in error. It is now appreciated that a light trapping effect must also be created in order to effectively absorb the longer wavelength light in the usable solar spectrum.

Development of the $(CdZn)S/Cu_2S$ has continued with direction to the research being provided by running a CdS/Cu_2S cell in parallel with the mixed sulfide cells. It has been found that the behavior of the mixed sulfide cell is particularly sensitive to the method of formation of the Cu_2S layer and the need for further structural characterization of this cell has been delineated.

In the area of theoretical analysis and modeling the effects of the two dimensional current flow in the Cu_2S layer is being explored in detail. Preliminary results indicate that significant errors in assigning fundamental mechanisms to the observed macroscopic current voltage behavior can occur when using the published approximate solution to the current flow problem. Further direct measurements of the interface velocity on a range of cells are reported using the analysis which couples light capacitance and spectral response.

The changes in short circuit current which accompany the heat treatments have been shown to be related to changes in the absorption coefficient of the Cu_2S layer. The absorption coefficient variations are due to the degeneracy of the Cu_2S layer and the changes in the position of the Fermi level as the stoichiometry of the Cu_2S is modified by the presence of the Cu_2O layer on its surface.

A thorough review of the available information on cell encapsulation studies in the large scale silicon array program and other thin film studies indicates that an inorganic glass encapsulant is the only plausible route to adequate hermetic encapsulation for the CdS/Cu_2S cell. Experiments to produce hermetic encapsulants are being planned.

4.1 Task 1. Development of CdS/Cu_2S Solar Cells.

The major thrust of this task is to develop a high efficiency planar cell, capitalizing on the fact that such a junction has the potential for higher open circuit voltages. The junction formation process for the planar cell eliminates the front surface texturing and results in a major increase in photon loss. Accordingly a substantial effort has been devoted to developing appropriate anti-reflection coatings for use on the relatively smooth Cu_2S surface.

4.1.1 Achievement of Improved Open Circuit Voltages

The achievable open circuit voltage is reduced by the area of the actual heterojunction, A_J, according to the following relation,

$$\Delta V_{OC} = kT/q \ \ell n \ A_j/A_{\perp} \ ^{*}$$

where $(A_{\perp})$ is the projected area of the cell. At least two factors influence the junction area, namely the morphology of the front surface of the CdS and the production of Cu_2S down the CdS grain boundaries. The morphology of the CdS on a gross scale reflects the surface of the metallic substrate and on a fine scale it is affected by the hydrochloric acid etch normally used to texture the surface before reaction to Cu_2S. The gross morphology of the CdS surface can therefore be influenced by selecting either the matte or smooth side of the copper substrate. Prior experience has shown that the solution reaction to form the Cu_2S causes extensive intrusions of Cu_2S which add significantly to the junction area. Accordingly a series of experiments were

* The diode factor for heat treated high efficiency cells is always very close to 1.

carried out in which CdS was deposited on either the smooth or matte side of the copper substrate and the CdS surface was left in the as deposited state or textured in the conventional way. The Cu_2S was produced by either solution or solid state reaction. Table I shows representative results for the open circuit voltages achieved following these various preparation procedures.

Table 1

Substrate	ρCdS(Ω-cm)	Cu_2S Reaction	Substrate	CdS Surface	Voc	Voc'
744B	5.0	Solution	Rough	Textured	0.486	.501
744A	5.0	Solution	Rough	Non-Textured	0.491	.509
745A	3.6	Solid State	Rough	Non-Textured	0.533	.554
686	9.6	Solid State	Smooth	Non-Textured	0.564	.577

Voc' is the computed open circuit voltage at 26 mA/cm^2

Poor photon economy caused low short circuit currents and the voltages were adjusted to a constant current to permit direct comparison. It is seen that substantial changes in open circuit voltage occur with the highest voltage achieved corresponding to the junction which would be expected to have the minimum area.

It must be stressed that these comparisons can only be conducted with essentially equivalent CdS layers. The resistivity of the CdS layer profoundly influences the achievable open circuit voltage and would tend to mask the voltage changes seen in the table if this parameter was not controlled.

All CdS substrate material for the above tests were subject to the established screening procedure covering resistivity, photoluminescence behavior, and morphology as observed in the scanning electron microscope.

4.1.2 Photon Economy Experiments

The low photon loss in the textured cell is in part due to the anti-reflection effects of the textured surfaces. The high index of refraction of Cu_2S will produce major first surface reflection losses with a planar surface and it has been clear for some time that the planar cell will require development of a good anti-reflection technology. A single layer anti-reflection coating can in principal achieve zero reflection at one specific wavelength but in the absence of texturing it would not be expected to achieve the low photon losses required for high efficiency cells. By using two layers it is possible in principal to achieve zero reflectance at two wavelengths. By appropriately positioning these in the active photon range of the solar cell one can anticipate achieving the low overall reflectance of less than about 5% which is desired. Theoretical analyses coupled to experimental measurements have been carried out during this quarter in an attempt to develop a satisfactory anti-reflection technology.

Two layer coatings previously reported in Ref. 1 showed the expected double minima for experimental cells and for theoretical calculations using a plane parallel layer approximation. It was, however, pointed out in that work that the Cu_2S layer thicknesses used in the experimental cells were substantially larger than the values expected to be optimum for overall cell performance. Measurements conducted during this quarter on cells with Cu_2S thicknesses that have been shown to give high efficiency revealed that the expected double

minima were not occuring. Accordingly, a computer analysis was carried out to determine the reflectance behavior that would be expected for an idealized cell in which all the layers are planar and parallel and for Cu_2S thicknesses that cover the useable range. Figure 1 shows a computed curve for the total reflectance from such an ideal cell with a double layer ZnS/MgF A-R coating. This curve is computed using published values of the Cu_2S absorption coefficient and values for the CdS layer measured at IEC. Normal incidence is assumed. It is immediately apparent that the desired first minimum at about 500 nm is being achieved but that there is almost no indication of the second minima which should occur at about 750 nm. To determine the origin of this effect, a second computation was carried out for the first surface losses only, it being assumed that all light that enters the cell is fully absorbed. The result is also shown on Figure 1 and does indeed reveal the anticipated double minima. It becomes obvious that the light reflected in the 750 nm region does not indicate the failure of a front-surface anti-reflection effect but is in fact light being reemitted from the cell after passage through the various layers and reflection from the metallic substrate. This effect would be reduced as the Cu_2S layer thickness increases as progressively more light would be absorbed during the two passes necessary before re-emission is possible. Indicated on the figure is the magnitude of the second minima reflectance for a range of Cu_2S thicknesses.

Curve 3 on Figure 1 is the experimentally measured reflectance for cell #757B12. This curve approximates reasonably well the shape which would be expected for a Cu_2S thickness of about 2500 Å. This cell which was produced by solid state reaction on CdS deposited on the smooth side of the substrate and had a measured Cu_2S thickness of about 1600 Å.

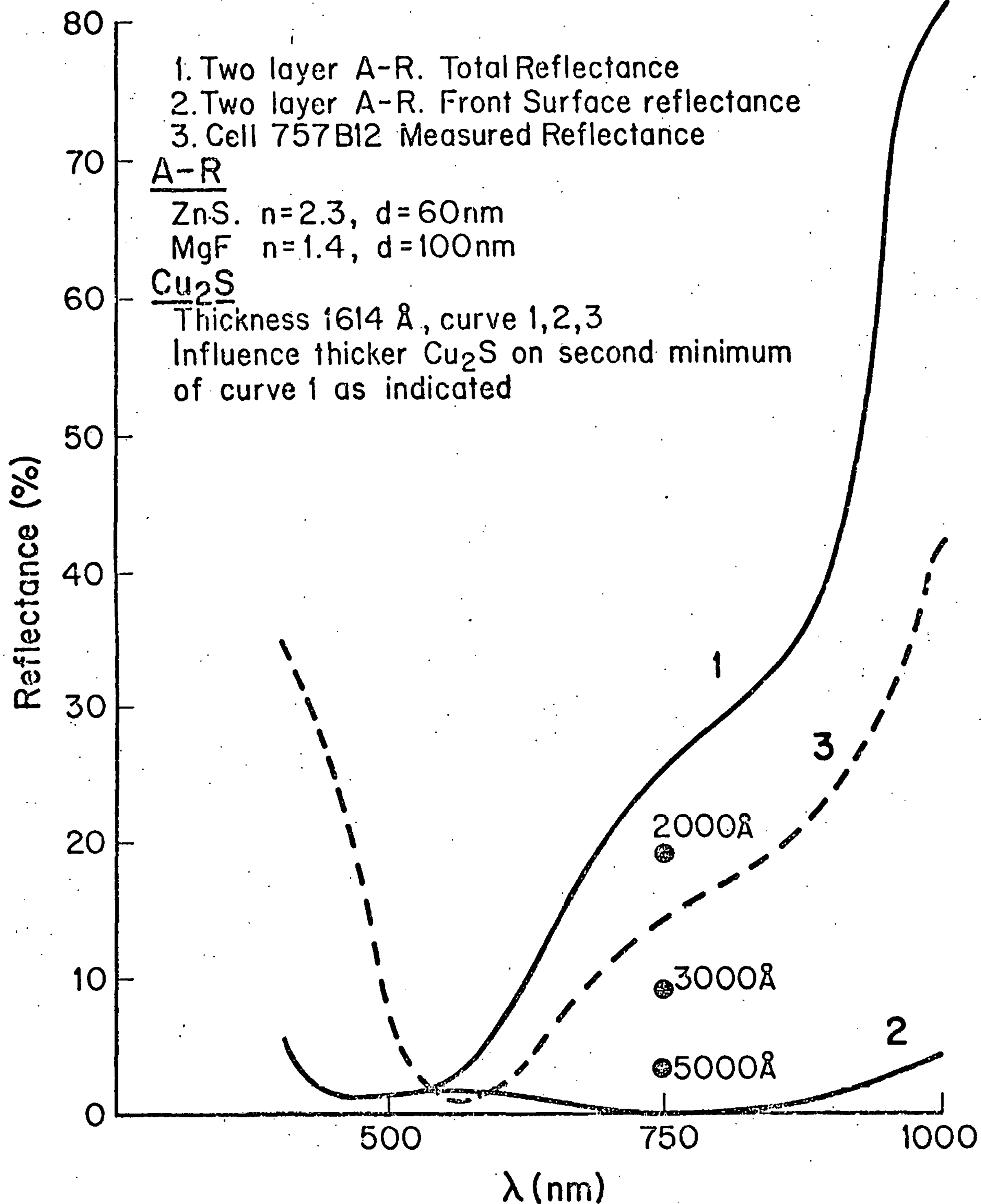

Fig. 1 The influence of a two layer A-R coating on total reflectivity from a planar junction CdS/Cu_2S solar cell. Theoretical and experimental results.

The significance of these observations and calculations is that the required photon economy cannot be achieved by merely applying anti-reflection coatings to the front surface of a planar junction CdS/Cu_2S cell. A significant portion of the useable light above a wavelength of 500 nm is not absorbed by two passes through the Cu_2S which is limited in thickness by the achievable minority carrier diffusion length. It has become clear that the high photon economy of the textured cell was in substantial part due to light trapping induced by the topography of front Cu_2S surface which results in multiple light passes through the active layer. During the coming quarter the options to induce the same degree of light trapping without reverting to a high junction area will be explored and steps taken to implement the concepts developed.

The original program plan for this task envisioned a limited development effort to achieve conventional two layer anti-reflection coatings on the CdS/Cu_2S cell. It is now seen that significantly more effort will be necessary to achieve the photon economy that previously resulted from light trapping in the Cu_2S and the development of the total anti-reflection system will take longer than initially expected.

4.2 Development of $(CdZn)S/Cu_2S$ Solar Cells

Work conducted under the previous contract established a reproducible system for depositing (CdZn)S layers of controlled composition and resistivity. During the present program it is intended to run a CdS substrate in parallel with a (CdZn)S substrate in order to provide base line data for comparison.

4.2.1 Influence of the Cu_2S Formation Process on Cell Properties

A sequence of cells was made on (CdZn)S substrates with approximately 19% zinc composition and on CdS substrates run in parallel. Comparison of the resulting cells has revealed a number of first order effects which will be investigated further during the coming quarter. Table 2 gives the measured current-voltage properties of the cells and also data such as the light and dark capacitance. The performance of these cells has not been fully optimized and no anti-reflection coatings were applied, which has a particularly strong effect on the currents and hence on the measured efficiencies.

The listed parameters indicate significant differences in the junction structure for the (CdZn)S as compared to the CdS. The dark capacitances for the (CdZn)S/Cu_2S cells are approximately twice those for the CdS/Cu_2S having the same treatment sequence. This could be interpreted as either a major difference in the junction area, or a consequence of slower diffusion of compensation copper into the (CdZn)S. The degree of change of the open circuit voltage in the (CdZn)S as the junction formation procedure changes is much more dramatic than for the CdS. This suggests that the morphology of the junction formed on the (CdZn)S is much more sensitive to the formation procedure than is the CdS. All the fill factors for the (CdZn)S/Cu_2S cells are less than for the CdS/Cu_2S cells and associated with this are higher shunt conductances. Previous experience with the CdS cell has shown that high shunt conductances are related to defects in the Cu_2S layer and it remains to be established whether the same is true for the (CdZn)S cell.

Total reflection measurements were made on the various cells and are shown in Figure 2. There are only small differences seen between the textured

Table 2

CdS/Cu_2S and $(CdZn)S/Cu_2S$ Cell Data

Cell Formation						
Cu Substrate	Smooth		Matte		Matte	
CdS Surface	Smooth		Smooth		Textured	
Cu_2S Formation	Solid State		Solid State		Solution	
Zinc Content	0	18%	0	19%	0	19%
Cell Number	M161	M160B	M155A	M154A	M155B	M154B
Component Properties						
Resistivity($\Omega \cdot cm$) CdS or (CdZn)S	2	20	6	15	6	15
Cu_2S Thickness (Å)	900	490	2180	1370	3146	2480
Cell Properties						
V_{OC}(V)	.506	.682	.500	.655	.501	.616
J_{SC}(mA/cm^2)	10.0	7.7	11.0	9.35	14.5	10.8
FF (%)	71.3	60.9	69.1	66.0	71.1	66.0
η (%)	3.61	3.21	3.82	4.05	5.18	4.37
$G_{SH}(\Omega \cdot cm^2)^{-1}$ x 10	1.24	2.77	1.76	2.62	1.98	3.11
C/A Dark(nF/cm^2)	6.1	11.0	7.2	18.0	16.0	33.0
C/A A.M.1(nF/cm^2)	95	55	59	65	74	93

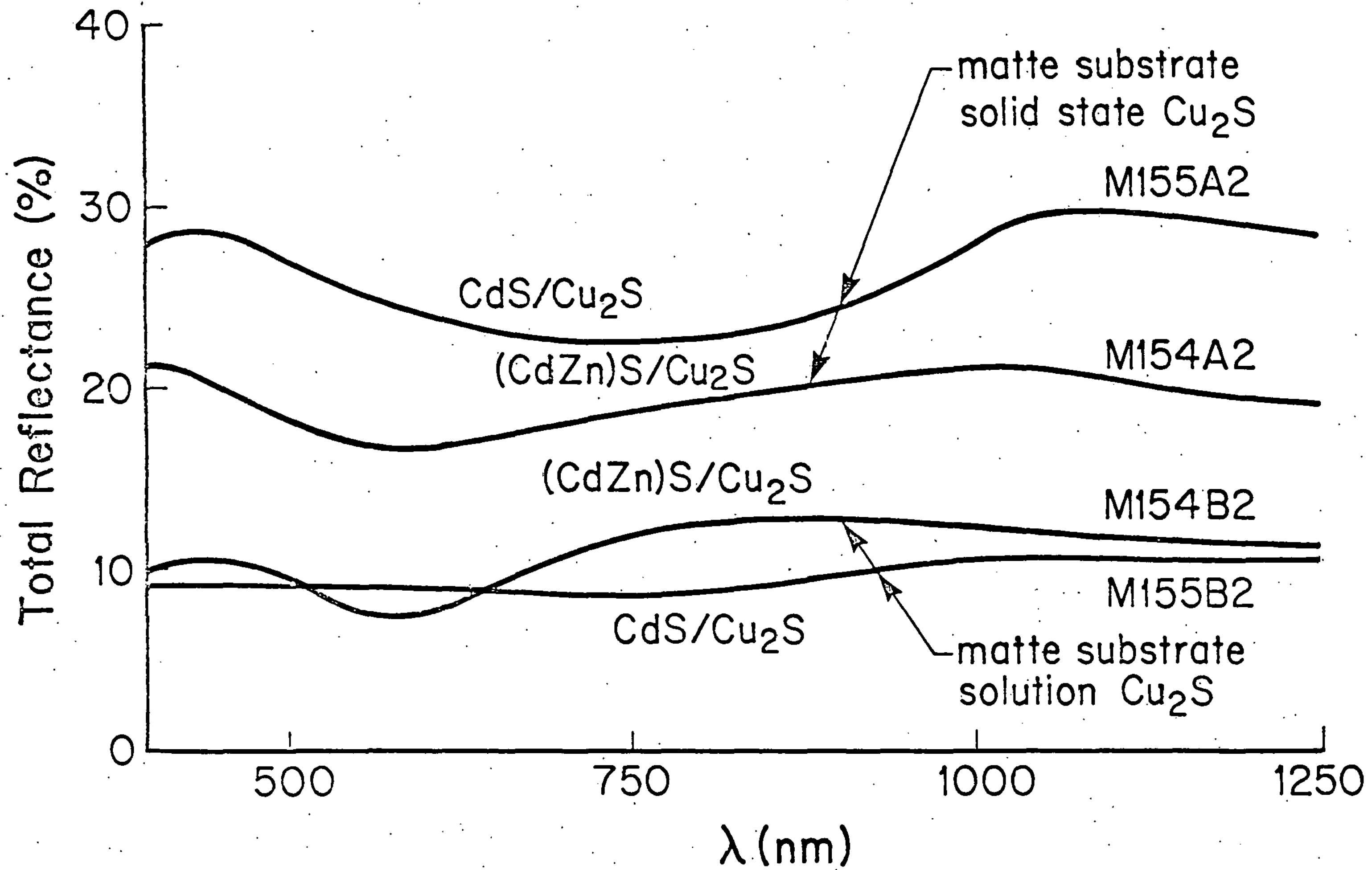

Fig. 2 Total reflectance from CdS/Cu_2S and (CdZn)S/Cu_2S Solar Cells

CdS and (CdZn)S cells but a more substantial difference is seen for the cells produced by the solid state process. As anticipated the total reflectance from smooth layers of Cu_2S are very high. The observed difference between the CdS and (CdZn)S cells has no immediately obvious explanation and will be further investigated.

4.2.2 Time Dependent Open Circuit Voltage

It has been reported in the past that the (CdZn)S cells sometimes but not always have open circuit voltages which decay with time. Until this period no substantial effort has been made to develop any systematic data on this effect. Experiments conducted with cells manufactured by the solution and solid state reaction have now been carried out and show quite substantial differences in behavior. Figure 3 shows the open circuit voltage decay for a number of cells that could be expected to have substantially different junction structure. It is seen that the more stable cells are those expected to have the most planar junction. This would suggest that the temperal instability is in some way related to the morphology of the junction and this point will be explored by in depth structural studies during the coming quarter.

4.3 Electro-Optic Analysis and Modelling

The routine testing of cells and the provision of feedback to the cell development efforts continues. During this quarter the analysis and experimental studies of collection efficiency effects in the CdS/Cu_2S cell were summarized and prepared for publication. The deduced interface recombination rates are in agreement with published analyses which are, however, relatively simplistic. In the area of theoretical modelling and analysis a rigorous analysis of two dimensional current flow in the Cu_2S layer has been

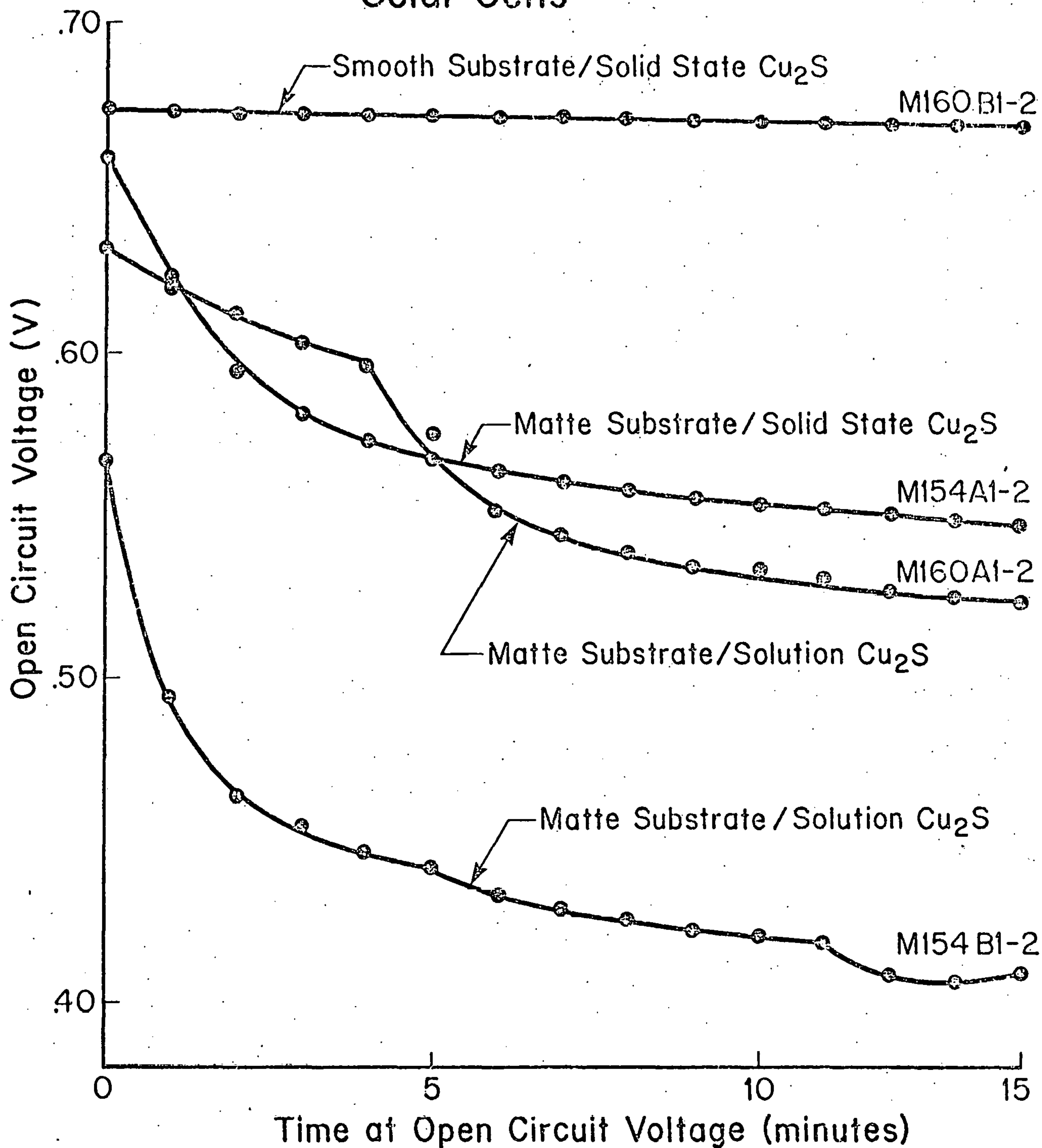

Fig. 3 Time dependent decay of open circuit voltage for (CdZn)S/Cu_2S Solar Cells of Various Designs.

started. The influence of stoichiometry on the optical behavior of Cu_2S and the associated changes in cell behavior have been analyzed theoretically and the results of the analysis applied to available experimental data.

4.3.1 Two dimensional Current Flow in the CdS/Cu_2S Cell

In the previous report it was shown that a lumped circuit analysis of the current voltage behavior of a typical CdS/Cu_2S cell, while mathematically possible in terms of linear series and shunt resistances, gave physically unacceptable parameters. In order to explore the reasons for this a complete two dimensional analysis of current flow in the Cu_2S layer is being conducted. During this quarter it has been shown that published analyses of the relation between sheet resistance and fill factor are approximations to the exact relations. The recent analysis by Wyeth[2] gives the following relation

$$R_S = R_{\square} L^2/12$$

where R_S is the measured series resistance, $R_{\square}$ the true sheet resistance and L the spacing of a simple parallel grid. This relation is strictly correct only at the open circuit voltage point. The earlier analysis by Wolf[3] which leads to the relation

$$R_S = R_{\square} L^2/8$$

is strictly correct only at a current value equal to the light generated current or at approximately the short circuit position. Table 3 reveals the sensitivity of the fill factor calculated from these approximate relationships and the exact value, at various sheet resistances.

Table 3

Comparison of Influence of Sheet Resistance on Fill Factors Calculated Using an Exact Analysis and the Approximations of References 2 and 3

Sheet Resistance $R_\square$ ($\Omega/\square$)	Fill Factor (%) Exact	Ref. 2	Ref. 3
6.0×10^3	78.4	77.6	78.5
2.5×10^4	72.1	69.3	72.9
5.0×10^4	63.6	58.8	65.7

It is seen that quite significant errors would be introduced, particularly at high sheet resistances.

During the course of this analysis it became clear that a totally independent way of measuring the sheet resistance of the Cu_2S layer on an active cell would be of great benefit. An interdigitated grid has now been designed and masks ordered which will allow this type of measurement to be made and will also allow operation of the cell in a normal manner. The significance of the results obtained to date is that utilizing the conventional lumped circuit analysis to deduce the linear resistance terms can lead to a deduced shunt resistance which does not in fact have any physical reality. It would clearly be undesireable to base cell improvement measures on such erroneous conclusions.

4.3.2 The Influence of Cu_2S Stoichiometry on Optical Absorption

Data exists in the literature (4,5) indicating that the absorption coefficient of Cu_2S varies with stoichiometry. There is abundant data[6] indicating that the short circuit current of the CdS/Cu_2S solar cell varies with the stoichiometry of the Cu_2S layer. From previous work[7] it is known that the stoichiometry of the Cu_2S layer can be varied by oxidation in air

or reduction by heating in a reducing atmosphere. Changes in both sheet resistance and short circuit current accompany these treatments. The purpose of the work reported here is to explore the relation of the absorption coefficient of Cu_2S and its carrier density, and the relation to the sheet resistance of the layer.

The effect which is most likely to cause changes in the Cu_2S absorption coefficient as its carrier density changes is the Burstein-Moss shift[8] which occurs in a degenerate material. It is basically a shift in the effective band gap of the semiconductor. In general, one expects that the absorption coefficient can be written as[9.10]

$$\alpha(h\nu) = A(h\nu)\,(h\nu - E_g - B_s E_F')^s \qquad (1)$$

where $\alpha(h\nu)$ is the wavelength or photon energy dependent absorption coefficient $A(h\nu)$ a wavelength dependent factor, $h\nu$ the energy of the incident photon, E_g the band gap of the absorbing semiconductor, E_F' the position of the Fermi level above the conduction band minimum in n-type material or below the valence band maximum in p-type material, B_s a constant which depends upon the effective masses[6] and s an exponent which is 1/2 for direct gap material and 2 for indirect gap material.

The relation between E_F' and the carrier density is through the Fermi integrals[11]

$$p = N_v F_{1/2}(E_F'/kT) \qquad (2)$$

where N_v is given by $N_v = 4.83 \times 10^{15}\, T^{3/2}\, (m_v^*/m_o)^{3/2}$ and $F_{1/2}(E_F'/kT)$ is tabulated function.[8] For Cu_2S, m^*_v/m is not known accurately[12], hence a value of unity is a reasonable starting assumption.

The resistivity of non-degenerate semiconductors is related to the carrier concentration through the relation

$$\rho = (q\,\mu\,p)^{-1} \qquad (3)$$

where q is the electronic charge and μ the mobility, which may itself be dependent upon the carrier density. In the carrier density range of interest $p > N_v \sim 2 \times 10^{19}/cm^3$, $\mu_p \sim \mu_0 (p/p_0)^{-.25}$ has been reported[12] with $\mu_0 \sim 5\ cm^2/V\text{-sec}$ and $p_0 = 10^{19}/cm^3$. This apparent variation may be due to applying Eq. (3) in the region of degeneracy where it is not valid. Since this empirical relation exists and is seen by other workers[13] we can use it without inquiring as to its fundamental cause[4].

From the form of Eq. (1) independent of the value of s there will be a cutoff wavelength above which α should fall to zero. This cutoff wavelength is given by

$$\lambda_c = 1.24/(E_g + B_s E_F') \tag{4}$$

with λ_c in μm and E_F' in eV. If no other absorption process occurred Eq (4) could be used to determine $B_S E_F'$. Unfortunately free carrier absorption[4,10] which occurs for $E_F' > 0$ and rises as λ^m with $m \simeq 2\text{-}3$ obscures the cutoff of the band to band transitions.

In order to see how $\alpha(h\nu)$ is expected to vary with carrier concentration or ρ we calculated the variation of α with ρ using Eq. (1) with $A(h\nu)$ = constant $B_s = 1$ and ρ determined by the empirical relation

$$\rho = \frac{7.42 \times 10^{-2}}{(\rho/Nv)^{3/4}} = \frac{7.42 \times 10^{-2}\ \text{ohm-cm}}{[F_{1/2}(E_F'/kT)]^{3/4}} \tag{5}$$

Fig. 4 shows the variation ρ, p and $\alpha(E_F')/\ \alpha(E_F = 0)$ at $\lambda = 0.75\ \mu m$ for $s = 1/2$ and $s = 2$. In fig. 5-7 we have plotted the calculated results in the form ρ/d versus α, with $d = 1.5 \times 10^{-5}$ cm and $A(h\nu) = 10^5$ for $\lambda = 0.65\ \mu m$, $0.75\ \mu m$, $0.85\ \mu m$, and $s = 1/2$ and $s = 2$, along with absorption and sheet resistance data deduced from the work of Windawi[5]. The value $A = 10^5$ gives the right order of magnitude for α and agrees with the theoretical estimate for the $s = 1/2$ case[14].

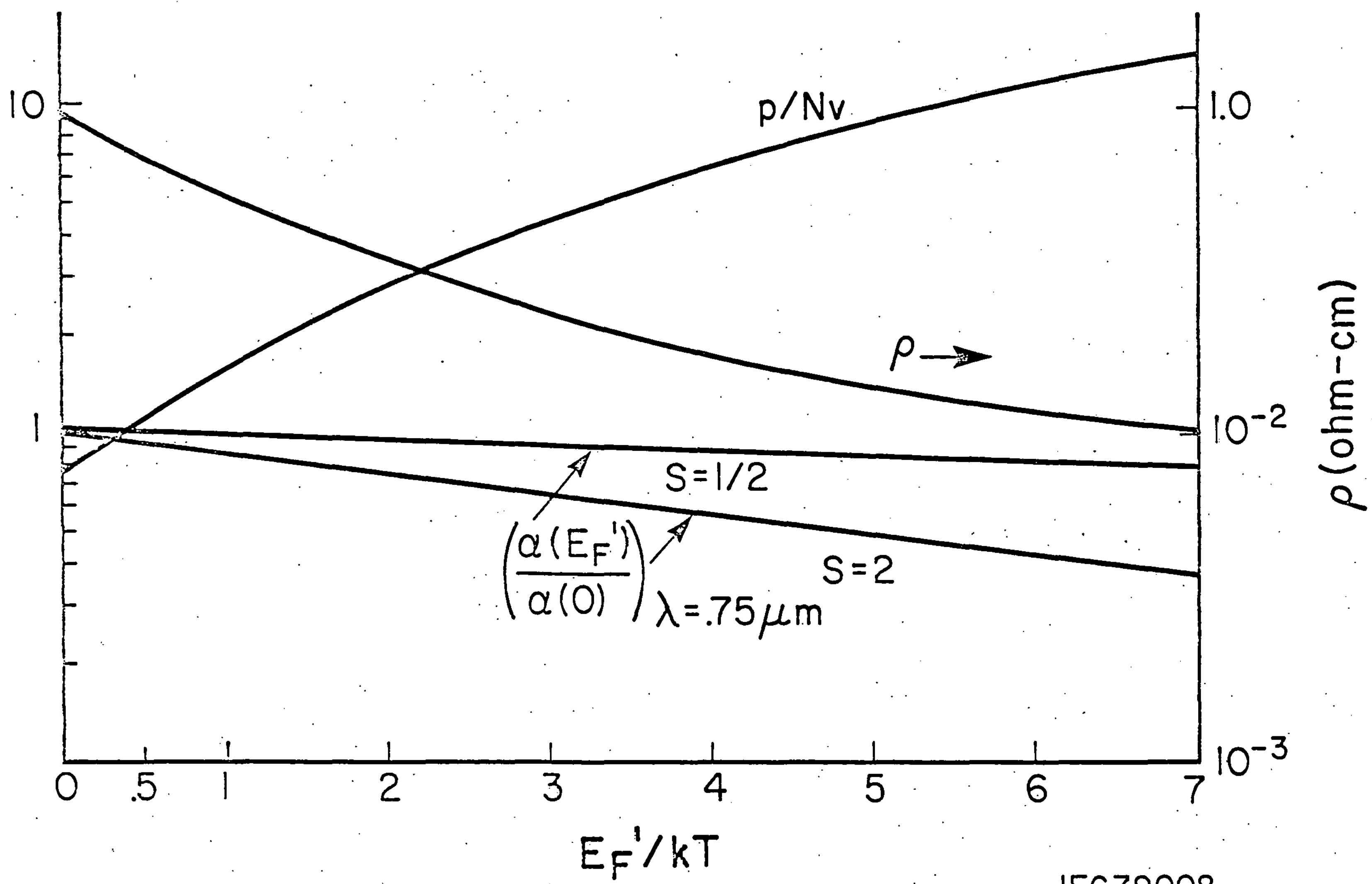

Fig. 4 Calculated variation of carrier density (p/Nv), resistivity (ρ) and normalized absorption coefficient ($\frac{\alpha(E_F')}{\alpha(o)}$) as a function of the position of the Fermi level (E_F').

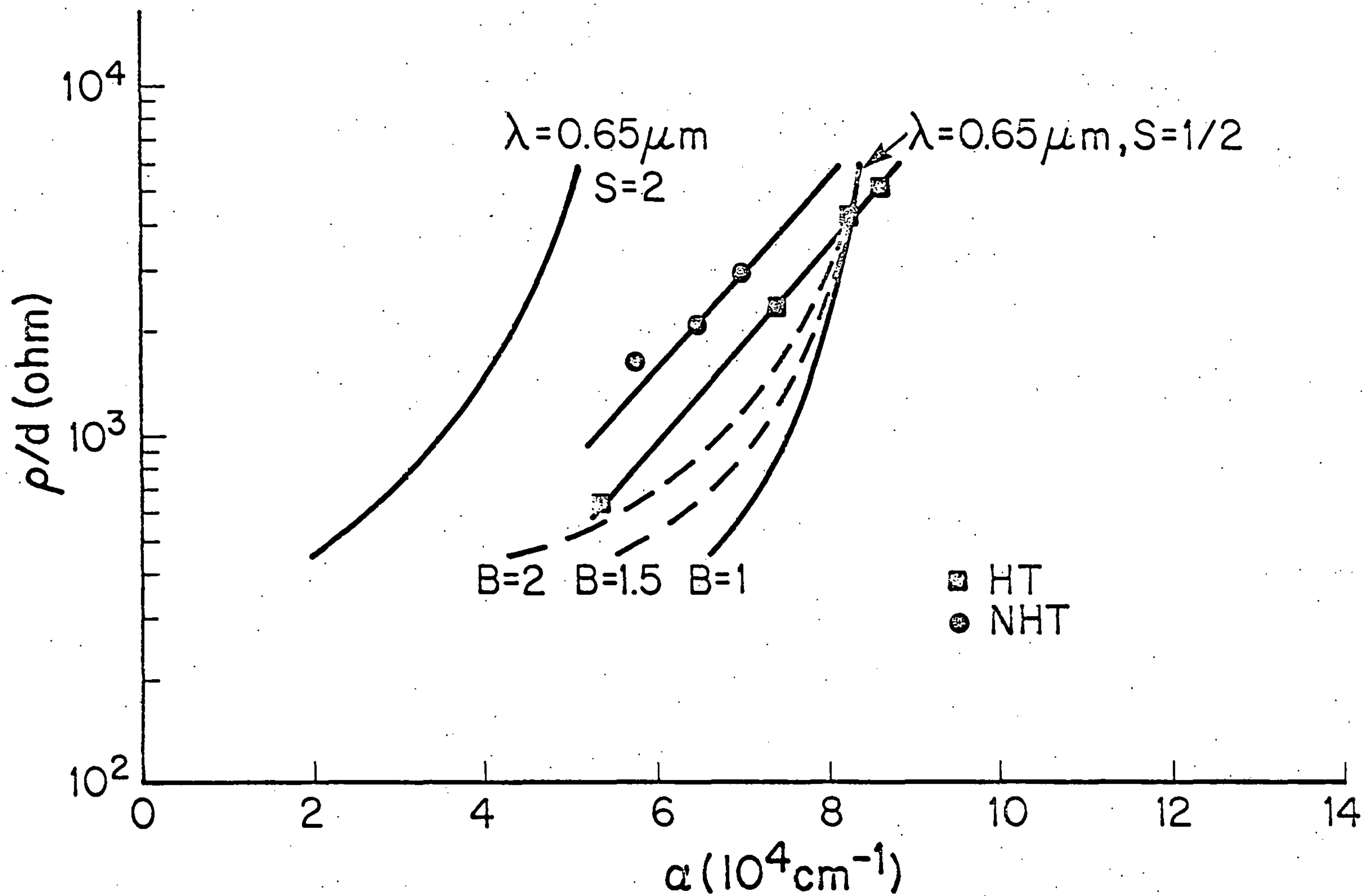

Fig. 5 Calculated sheet resistance as a function of absorption coefficient and experimental data points from reference 5. Corrected for absorption in CdS and reflection losses. Wavelength 0.65 μm. (NHT - immediately after Cu_2S formation. HT - heat treated in air at 250°C)

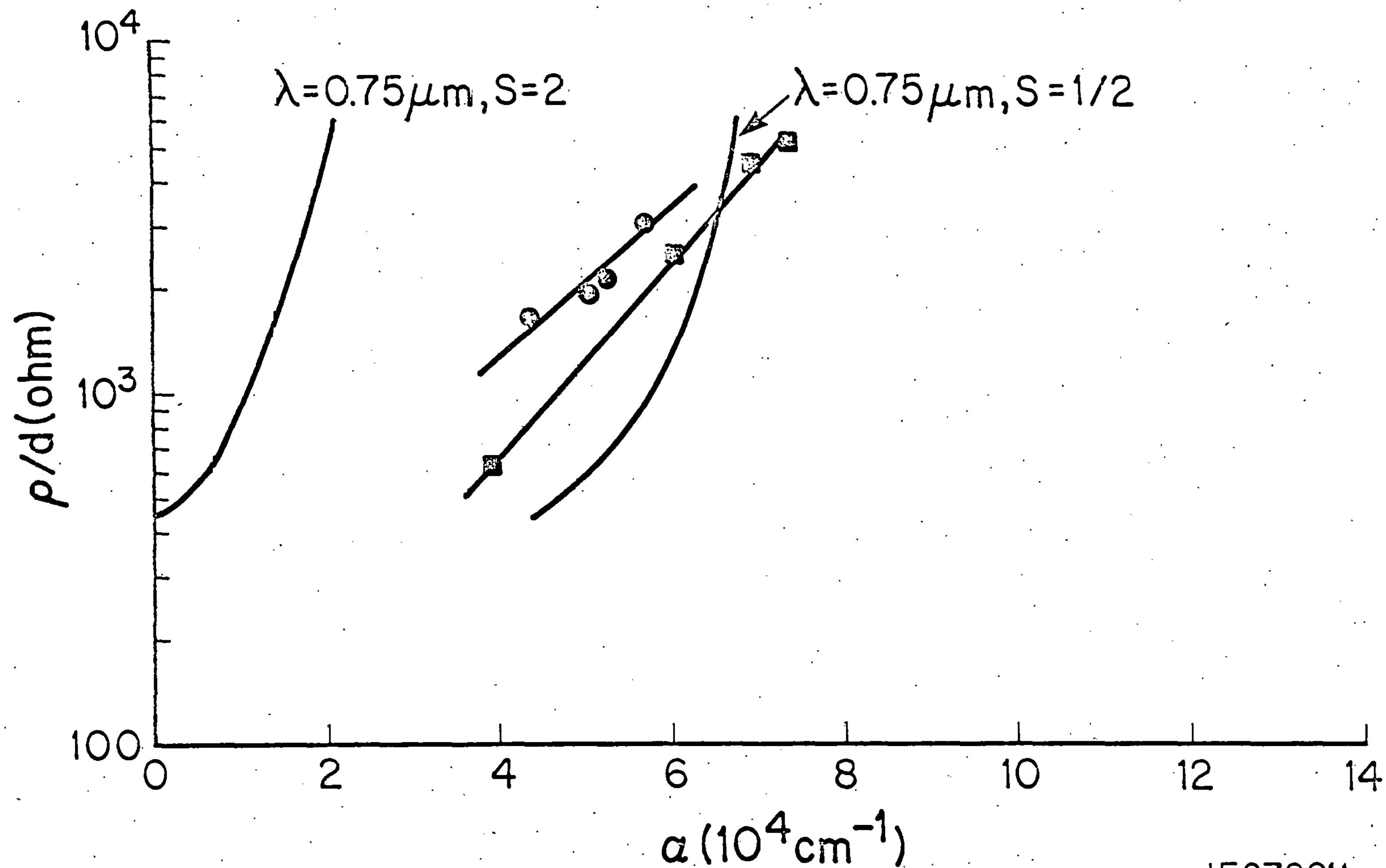

Fig. 6 Calculated sheet resistance as a function of absorption coefficient and experimental data points from reference 5. Corrected for absorption in CdS and reflection losses. Wavelength 0.75 μm.

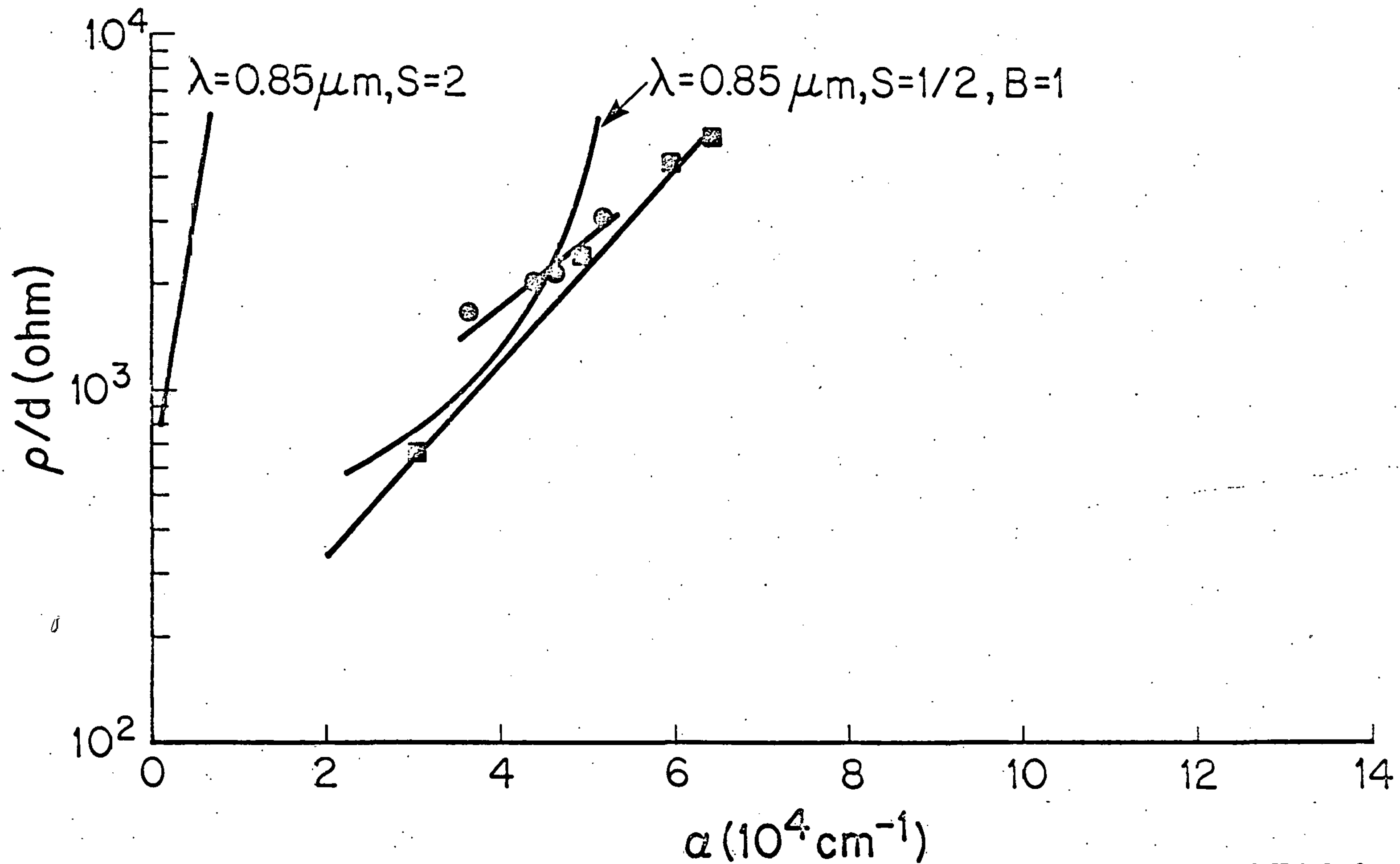

Fig. 7 Calculated sheet resistance as a function of absorption coefficient and experimental data points from reference 5. Corrected for absorption in CdS and reflection losses. Wavelength 0.85 μm.

calculation using an AM 1.5 spectrum indicated that a 50% decrease in α at all wavelengths would reduce the short circuit current by ~25%. In actual cells heating in air which leads to low ρ/d values, reduces j_{SC} by as much[16] as 40%. Some of this decrease may be associated with changes in diffusion length or interface properties. However, it is clear that a substantial part of the loss results from changes in the absorption coefficient.

4.3.3 Measurement of Interface Recombination Velocity in CdS/Cu_2S Heterojunctions

The determination of the interface recombination velocity by the analysis of intensity-capacitance and intensity-collection efficiency data has been applied to a number of CdS/Cu S cells. This work has been published and is appended to this report.[17] It has been found that interface recombination velocity which would be deduced from a relatively simple analysis of lattice misfit appears to apply to actual cells. Further refinements have been made to the experimental set-up to give continuous monitoring of the illumination intensity falling on the cell. This technique is a particularly powerful tool for exploring the detailed behavior of the junction region in both the CdS/Cu_2S and $(CdZn)S/Cu_2S$ cell and further studies will be carried out.

4.3.4 Trap and Defect Levels in CdS

In order to gain further insight into the behavior of the trap levels on the CdS side of the junction the available transient and thermally stimulated capacitance techniques are being reviewed. It is anticipated that a technique or a combination of techniques will be identified which will be applicable to the CdS/Cu_2S cell.

4.4 Encapsulation for Improved Stability

The past reports from the L.S.S.A. project have been reviewed and current reports are monitored as they are issued. The preliminary conclusion is that only an inorganic glass will combine total hermetic sealing, high transmissivity and residence to long term weathering and degradation. Accordingly non integral encapsulation experiments will be carried out behind sheet glass and a design for a suitable enclosure is now in preparation.

The possible techniques for applying an integral encapsulant include electron beam evaporation and sputtering. The former requires a suitable foil or powder as starting stock and sources for these are now being identified.

A support structure for roof top exposure of cells has been assembled. This will allow easy insertion and removal of cells under test to permit periodic measurement agreement on the solar simulator.

5. Future Developments

The major thrust in the CdS/Cu_2S task will be aimed at producing light trapping in an effectively planar Cu_2S layer. Two approaches appear to merit investigation. The first is to texture the surface of a layer deposited on top of a planar Cu_2S layer. This could be for example a final encapsulating glass layer. An alternative approach would be to texture a smooth metallic substrate on a scale sufficiently fine so that the surface of the deposited CdS remains essentially smooth.

Cell development efforts will continue on the $(CdZn)S/Cu_2S$ junction with particular attention being focused on the structure of the junction and its effect on cell behavior.

Experimental and theoretical analysis of the achieved photon economy will continue with the planar CdS/Cu_2S cell. Understanding and control of the hole traps will be sought using both photoluminescence and transient capacitance techniques.

Trial encapsulations will be made on CdS/Cu_2S cells and the resulting optical and electronic effects measured.

References

1. I.E.C. Final Report. EG-77-C-03-1376-FR.
2. N. C. Wyeth, Solid State Electronics, 20, 629, (1977).
3. M. Wolf, Proc. IRE, 48, 1246, (1960).
4. V. P. Kryzhanovskii, Optics and Spectroscopy 24, 135-137, (1968).
5. L. C. Burton and H. M. Windawi, J. Appl. Phys. 47, 4621-26, 1976.
6. Palz et al. Proceedings of 9th IEEE Photovoltaic Specialists Conference Silver Spring, MD, May 1975, p. 91.
7. Baron et al., Proceedings of 13th IEEE Photovoltaic Specialist Conference Washington, D.C. June 1978, p. 406.
8. E. Bustein, Phys. Rev. 93, 632 (1954).
   J. S. Moss, Proc. Phys. Sco. (London) B76, 775 (1954).
9. V. I. Fistul, "Heavily Doped Semiconductors," Plenum Press, NY, 1969.
10. J. I. Pankove, "Optical Processes in Semiconductors," Prentice-Hall, Inc. Englewood Cliffs, NJ 1971.
11. J. S. Blakemore, "Semiconductor Statistics" Pergamon Press, NY, 1962.
12. F. Guastavino, H. Luquet, J. Bougnot, Proc. of Photovoltaic Power and its Applications in Space and on Earth. International Congress The Sun in the Service of Mankind, Paris, 1973, p. 189.
13. N. A. Vlasenko, Ya. F. Kononets, Ukranian Physics Journal 16, 237-243, 1971 (Translation p. 284-292).
14. T. S. Moss, G. J. Burrell, B. Ellis, "Semiconductor Opto-Electronics," John Wiley and Sons 1973.
15. L. R. Shiozawa et al Clevite Report Contract AF33, 615-5224, June 1966-May 1969.
16. A. Rothwarf, 1979 Photovoltaic Solar Energy Conference, Berlin, W. Germany April 1979.
17. N. C. Wyeth and A. Rothwarf, "Measurements of Interface Recombination Velocity by Capacitance/Collection Efficiency Variation in Cu_2S/CdS Heterojunctions," Journal of Vacuum Science and Technology (July 1979).

Appendix A

MEASUREMENTS OF INTERFACE RECOMBINATION VELOCITY BY CAPACITANCE/COLLECTION EFFICIENCY VARIATION IN Cu_2S/CdS HETEROJUNCTIONS

by

N. Convers Wyeth and A. Rothwarf

Institute of Energy Conversion
University of Delaware
Newark, DE 19711

ABSTRACT

The interface recombination velocity, S_I, in the Cu_2S/CdS heterojunction has been measured by a new technique using junction capacitance and collection efficiency. The method capitalizes on changes in the junction field strength due to the photo-charging of traps in the depletion region, as measured by junction capacitance. The variation in junction collection efficiency is related to the field strength changes to obtain S_I values of order $\sim 3 \times 10^5$ cm/sec. These compare well with estimates from other experiments and simple theoretical predictions. This measurement technique could be applied to other systems.

Accepted for publication in Proceedings of the Sixth Annual Conference on the Physics of Compound Semiconductor Interfaces (Journal of Vacuum Science and Technology 16, July/August 1979)

I. INTRODUCTION

The Cu_2S/CdS heterojunction is currently being studied for its promise as a low-cost, thin film photovoltaic solar cell. The p-Cu_2S is degenerate and the junction space-charge region lies almost entirely in the n-CdS. In operation photo-generated electrons in the Cu_2S diffuse to the junction and are swept into the CdS by the field to become majority carrier current flow. Any loss of these carriers by recombination at the interface directly diminishes the output current. Hence measurement of the interface recombination velocity and its dependence on cell formation conditions is important to the achievement of improved conversion efficiency. This interface is also attractive for basic studies because the Cu_2S is formed by a topotaxial ion-exchange process which produces the junction within the original bulk CdS and hence free of the usual surface contamination problems.

Heat treatments to optimize cell efficiency cause diffusion of Cu acceptors into the CdS junction region. Dark capacitance measurements show the expected increase in the space charge width. However under illumination the capacitance increases by up to two orders of magnitude, due to trapping of photo-generated holes by the Cu acceptors and the consequent increase in the CdS space-charge density. Thus, using the illumination intensity, the field strength at the junction can be varied over a wide range at a fixed junction bias voltage. By modeling the relations between the junction capacitance C, junction field F_2, and the current collection efficiency η_c, the value of the interface recombination velocity S_I can be deduced.[1,2] The values of S_I obtained, 10^5-10^6 cm/sec, support the hypothesis that the interface states are dangling bonds on the misfit dislocation that exist by virtue of the lattice mismatch across the interface.[3]

Although it is the particular defect structure of the Cu compensated CdS layer that makes the photocapacitance and collection efficiency of the CdS/Cu_2S junction so sensitive to light, similar defects could be introduced into other systems allowing this method of determining S_I to be applied.

II. THEORY

In semiconductor heterojunctions between materials which differ in lattice constant, there usually exists a network of misfit dislocations. The dangling bonds associated with these dislocations form the interface states. The total density per unit area of such states N_I is proportional to the difference in lattice constant, but the distribution of these states in energy is not known. Current flow across an interface can be dominated by the interface states. For the Cu_2S/CdS heterojunction with the band diagram illustrated in Fig. 1, the competing electron flow mechanisms from CdS to Cu_2S are (1) diffusion of electrons with energy above Ec_1; (2) recombination of electrons with energy at or above $Ec_2(x=0)$ through interface states, and (3) tunneling of electrons with energy less than $Ec_2(x=0)$ to interface states. Since $\Delta\chi \approx 0.2$ eV the density of electrons at the interface favor mechanisms (2) and (3). Mechanisms (2) and (3) yield the following expression for the current, in the dark, for an ideal junction (no series or shunt resistance effects):

$$\begin{aligned} I_1 &= A_j q\, Nc_2\, S_I \exp - \phi/kT(\exp \frac{qV}{kT} - 1) \\ &= j_o A_j\, [\exp(qV/kT) - 1] \end{aligned} \qquad (1)$$

where A_j is the junction area, q the electronic charge, Nc_2 the effective density of states at the CdS conduction band edge ($\sim 2 \times 10^{18}$ cm^{-3}), S_I the effective interface recombination velocity, and ϕ the effective barrier height given by

$$\phi = E_{g1} - \Delta\chi - V_{Dp} - \delta_1 \qquad (2)$$

with E_{g1} the bandgap of Cu_2S, $\Delta\chi$ the difference in electron affinity between Cu_2S and CdS, V_{Dp} is the band bending in Cu_2S and δ_1 the position of the Fermi

level relative to the Cu_2S valence band. (See Fig. 2)

In the Cu compensated region of CdS a number of defect levels lie above the Fermi level (see Fig. 2). The charging of these levels produces a time dependent experimental current-voltage (I-V) curve in the dark, with time constants on the order of hours. This effect makes the use of Eq. (1) for studies of S_I from the dark I-V inappropriate.

Under illumination the Cu_2S/CdS exhibits photovoltaic properties. The light generated current is produced primarily by the absorption of photons in the Cu_2S layer. However, the light reaching the CdS layer plays a very important role in "gating" the flow of electrons through the interface region. In steady state the injected electron current density, j_{LO}, the current density lost at the interface through interface recombination, j_{LR}, and the current density which passes through the external circuit, j_L, are determined through the relations

$$j_{LO} = j_{LR} + j_L, \tag{3}$$

$$j_{LR} = qn_I S_I, \tag{4}$$

and

$$j_L = qn_I \mu_2 F_2 = qn_I v_D \tag{5}$$

for $\mu_2 F_2$ less than the saturation velocity $v_D < v_{th}$ These equations can be solved to yield[2]

$$j_L = j_{LO} \frac{\mu_2 F_2}{S_I + \mu_2 F_2} \equiv j_{LO} \eta_I \tag{6}$$

with n_I the density of light injected electrons at the interface, μ_2 the mobility of electrons in CdS, and F_2 is the field at the interface and η_I the interface collection factor.

The full current-voltage relation under illumination is given by combining Eqs. (1) and (5) to obtain

$$I = I_1 - Aj_L \tag{7}$$

The junction field F_2 is directly related to the total positive charge stored in the CdS space charge region. Under illumination the deep compensating Cu centers store holes. The mechanisms leading to hole storage are illustrated in Fig. 2. The consequence of such hole storage is to shrink the width of the space charge region increasing the capacitance of the junction as illustrated in Fig. 2. Under the assumption of uniform density and charging of the deep levels under illumination the junction field is given by

$$F_2 = \frac{2\,V_D}{w} = \frac{2\,V_D}{\varepsilon\varepsilon_0}\,\frac{C}{A} \tag{8}$$

where V_D is the diffusion voltage, w the width of the space charge region under illumination, ε the dielectric constant of CdS (~ 10), ε_0 the permittivity of free space (8.85×10^{-14} F/cm^2), and C the total capacitance of the junction.

When the junction is illuminated with a known photon flux Φ, the collection efficiency η_c is given by $\eta_c = j_L/q\Phi$ and using Eq. (6) one can obtain a linear form for the relationship between F_2 and η_c. This relation is

$$F_2^{-1} = \frac{\eta_Q}{(S_I/\mu_2)}\,\eta_c^{-1} - \left(\frac{S_I}{\mu_2}\right)^{-1} \tag{9}$$

where $\eta_Q \equiv j_{LO}/q\Phi$ is the quantum efficiency of the cell and includes all photon and electronic losses other than those due to the interface. Both C and η_c change with light intensity. Eq.(9) when used to analyze the data yields S_I/μ_2 and η_Q.

III. SAMPLE PREPARATION

All samples were prepared on electroformed copper foil ∿ 25 μm thick, plated with ∿ 0.5 μm of Zn. CdS powder is evaporated from a graphite source at ∿ 1050°C onto the heated substrate ∿ 250°C. The CdS layer formed is ∿ 25 μm thick, has resistivity of 1 to 10 ohm-cm, with crystallite diameter 1 to 5 μm, and oriented with the c axis perpendicular to the substrate.

The Cu_2S layer is prepared either by dipping the CdS layer into a cuprous ion solution at ∿ 95°C for 5 to 10 sec, or by the deposition of CuCl onto the surface and heating for ∿ 2 min. at 200°C, followed by a rinse in water or methanol. For the first method the equivalent thickness of Cu_2S is ∿ 1500 - 3000 Å including material formed down grain boundaries to a depth of 1-2 μm. For the second method the thickness is 1000-1500 Å with little grain boundary formation of Cu_2S. The samples reported here were prepared on the smooth side of the electroformed copper with source temperature 1060°C, substrate temperature 205°C, CdS thickness 17 μm, CdS resistivity 2 ohm-cm, Cu_2S thickness 1200 Å by method two. Previous results[1] were for Cu_2S prepared by method one.

The top contact to the Cu_2S is a fine grid (32 lines/cm) evaporated through a shadow mask. The width of a grid line is 20 μm and its thickness 1-2 μm. A gold plated tab makes contact to the grid fingers.

In the process of optimizing cell efficiency the samples are subjected to heat treatments in CO, H_2-Ar, and vacuum (50 μm) at 170°C for a number of hours (10-100). These treatments convert the Zn plated substrate to brass, reduce Cu_2O on the surface to Cu, and diffuse Cu into the CdS layer. This last aspect can be seen by the steady decrease of the dark capacitance

as the Cu compensation progresses into the CdS layer. The initial value of the dark capacitance depends upon the resistivity of the CdS layer with typical initial dark C/A values of 50-100 ηF/cm^2; after heat treatment values of 1 - 10 ηF/cm^2 are seen in the dark. Capacitance values under illumination depend upon the intensity and spectral content of the light.

IV. EXPERIMENT

The basic measurements made are junction collection efficiency and junction capacitance as a function of illumination intensity. The cell under test is mounted on a temperature-controlled block (28°C) with an adjacent silicon monitor cell, and is illuminated through a diffuser by a tungsten ELH lamp to simulate AM1 spectral distribution. The intensity of light on the block is varied by interposing neutral density filters which preserve the relative spectral content transmitted. The short-circuit current of the silicon monitor cell varies linearly with intensity, as does the electron flux arriving at the junction from the Cu_2S. Thus a relative measure of the junction collection efficiency is obtained by dividing the Cu_2S/CdS cell current by the silicon cell current. The test cell is held at zero bias by a bipolar power supply and the current measured by an operational amplifier circuit.

The capacitance of the junction is measured using a phase-sensitive detection system[4] which can handle moderate parallel conductances. A small a.c. voltage (10 mV rms at 10 kHz) is applied to the cell through the bipolar supply and the 90° out-of-phase current component is measured by a lock-in amplifier. The capacitance is then easily calculated and normalized to the test cell area. The system is calibrated using a standard capacitor, and the measurements are reproducible to ∿ ± 1%.

At any given level of illumination, the capacitance of the junction can be measured as the bias is changed from zero using the bipolar supply. Thus plots of C^{-2} versus V can be obtained.

V. RESULTS AND ANALYSIS

The relative collection efficiency and capacitance for a range of illumination intensity were measured on three similar cells. A typical result is shown in Figure 3; for comparison with Eqs. (8) and (9) the reciprocal capacitance is plotted versus reciprocal collection efficiency. Note that if relative collection efficiency is used, η_Q cannot be found but the y-axis intercept will still yield S_I/μ_2. Figure 3 shows a linear region with a bending over at low intensities, indicating that the simple model breaks down as dark conditions are approached. Equation (8) assumed uniform space charge density. If a deep trap level exists in the CdS depletion region and crosses the electron quasi-Fermi level, its contribution to capacitance and junction field will vary as the width of the depletion region varies.(5) Such a level would also affect the capacitance-bias voltage relation. Figure 4 shows how the extrapolated voltage intercept from C^{-2} vs V plots moves from higher values toward the expected value of diffusion voltage V_D (0.6 - 1.0 volts) as intensity is increased. This is the predicted effect of a trap level crossing(5) and will be explored in detail in future work. It suffices for this work to note that where the linear behavior of C^{-1} vs. η^{-1} occurs, the values of V_D are reasonable and the assumption of a uniform space charge density in Eq. (8) is justified.

Table I shows the reduced data from the three cells from plots like Figure 3. The C^{-1} vs. η^{-1} occurs, the values of V_D are reasonable and the assumption of a uniform space charge density in Eq. (8) is justified.

Table I shows the reduced data from the three cells from plots like Figure 3. The C^{-1} axis intercept is found by extrapolating the linear region, S_I/μ_2 calculated through Eq. (8) with V_D = 0.9 volts, and S_I deduced assuming

$\mu_2 = 100\ cm^2/V\text{-sec}$.[6] The three cells shows relatively small variation among themselves. An estimate of S_I can also be made from the reverse saturation current, j_o, measured from the cell current-voltage characteristic. The relevant equations are (1) and (7). The measured values of j_o obtained under illumination are listed in Table I along with values of S_I calculated using Eqs. (1) and (2), assuming $V_{Dp} \approx 0$, $\delta_1 \approx 0$ and $(Eg_1 - \Delta X) \approx 1$ eV. The values of S_I from j_o are generally larger, indicating that a separate measurement is needed to determine ϕ accurately. Either internal photoelectric emission from the Cu_2S to the CdS at the interface is used, or the temperature variation of j_o.

It should also be noted that in some systems the interface recombination mechanism may not dominate the diode equation, i.e. drift and diffusion of carriers to the interface may be the rate limiting step.[7] In such systems the variation of j_L with field may be the only reliable technique available.

A further point to consider is that for the values of S_I obtained the upper limit on S_I of $\bar{v}/4$ is being approached, at which all the carriers with velocity components toward the interface are captured and recombine there.

A simple theoretical model[8,9,10] can be used to estimate S_I for a given heterojunction from the lattice mismatch. The expression is

$$S_I = N_I^* V_{th}\, \sigma \qquad (10)$$

where N_I^* is the density of interface states effective in the recombination process, σ is the mean capture cross section of the interface states, and V_{th} the thermal velocity of the electrons. Using[10] $N_I \approx 2\Delta a/a^3$ with Δa the

difference in lattice constant across the interface and a the average lattice constant, the 4-5% lattice mismatch in the CdS/Cu_2S system yields $N_I \approx 5 \times 10^{13}/cm^2$. Estimates[8] give $\sigma \approx 10^{-14} - 10^{-15}/cm^2$. Hence with $v_{th} \approx 10^7$ cm/sec, S_I is expected to be in the range $5 \times 10^5 - 5 \times 10^6$ cm/sec. The observed values are indeed within this range.

From Eq. 10 one can write

$$S_I \approx \frac{2 \sigma v_{th}}{a^2} \frac{\Delta a}{a} = v_o s . \qquad (11)$$

Since σ and the lattice constants vary only slightly, v_o should be nearly independent of materials; thus S_I will vary linearly with s, the strain across the interface due to lattice mismatch. Support for such an hypothesis is obtained from adding our results to those of Ettenberg and Olsen[4] on the $In_xGa_{1-x}P/GaAs$ system as shown in Figure 5.

VI. SUMMATION

A new method of measuring interface recombination velocity has been described, and its application to an important heterojunction system demonstrated. Values measured by this technique agree with other experimental and theoretical estimates. The method capitalizes on the changes in junction field strength which can be obtained by photo-charging depletion region traps, and thus can in principle be applied to other systems in which such traps are present or can be introduced.

ACKNOWLEDGEMENTS

The contributions of R. F. Wieland in equipment construction and M. G. Cimorosi in data taking and analysis were very important in the progress of the experiments. This work was supported by the Department of Energy.

REFERENCES

1. A. Rothwarf, J. Phillips, N. C. Wyeth, Thirteenth IEEE Photovoltaic Specialists Conference - 1978 (IEEE, New York, 1978) p. 399.

2. A. Rothwarf, A. M. Barnett, IEEE Trans. Elec. Dev. ED24, 381 (1977).

3. M. Ettenberg, G. H. Olsen, J. Appl. Phys. 48, 4275 (1977).

4. J. Shewchun, A. Waxman, Rev. Sci. Instr. 37, 1195 (1966).

5. A. M. Goodman, J. Appl. Phys. 34, 329 (1963).

6. L. L. Kazmerski, W. B. Berry, C. W. Allen, J. Appl. Phys. 43, 3515 (1972); 43, 3521 (1972).

7. C. Wagner, Phys. Z, 32, 641 (1931); W. Schottky, E. Spenke, Wiss. Veroff. Siemens-Werken 18, 225 (1939); S. M. Sze, "Physics of Semiconductor Devices" (Wiley, New York, 1969); E. H. Rhoderick, "Metal-Semiconductor Contacts" (Clarendon Press, Oxford, 1978).

8. A. L. Milnes, D. L. Feucht, "Heterojunctions and Metal-Semiconductor Junctions" (Academic Press, New York, 1972) p. 57.

9. H. Kressel, J. Electron. Mater. 4, 1081 (1975).

10. A. Rothwarf, "International Workshop on Cadmium Sulfide Solar Cells and Other Abrupt Heterojunctions", University of Delaware, May 1975, NSF-RANN AER 75-15858, p. 9.

FIGURE CAPTIONS

Fig.1 Band diagram of the Cu_2S/CdS heterojunction (in the dark)

Fig.2 Band diagram of the CdS space charge region indicating optical processes which can produce hole storage in deep centers. (1) Band to band transition. (2) Valence band to unoccupied gap state, followed by center to valence band transition. (3) Direct excitation from center to conduction band. (4) Excitation from center to unoccupied gap state. Change in space charge region from dark to light and currents in light are also shown.

Fig.3 Reciprocal capacitance versus reciprocal collection efficiency (relative) for typical cell. The straight line was fitted to the linear region to allow extrapolation to $\eta^{-1} = 0$.

Fig.4 Variation of the extrapolated intercept of C^{-2} vs. V with illumination intensity for typical cell.

Fig. 5 Interface recombination velocity versus lattice parameter mismatch, including theoretical curve from Ref. 9, data from Ref. 3 on $In_xGa_{1-x}P/GaAs$, and the averaged data from the present work on Cu_2S/CdS.

Table 1. Values of S_I Calculated for the Four Cells Measured. S_I (C_o) Values Were Calculated Assuming μ_2 - 100 cm^2/V-s

Cell	$C_o(\eta^{-1} = 0)$ (nF/cm^2)	S_I/μ_2 (V/cm)	S_I (C_o) (cm/sec)	j_o (mA/cm^2)	S_I (j_o) (cm/sec)
M161B1-1	.672	1.37×10^3	1.37×10^5	3.17×10^{-8}	5.0×10^6
M161B1-2	1.83	3.70×10^3	3.70×10^5	3.54×10^{-8}	5.6×10^6
M161B1-4	2.22	4.48×10^3	4.48×10^5	6.29×10^{-8}	9.9×10^6

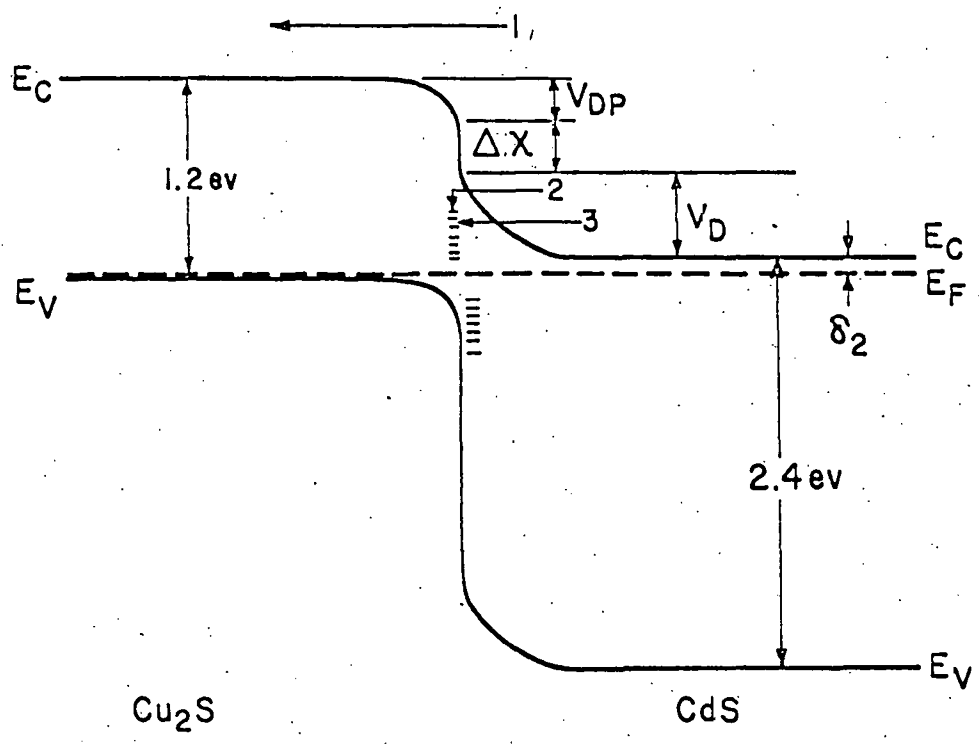

Fig. 1

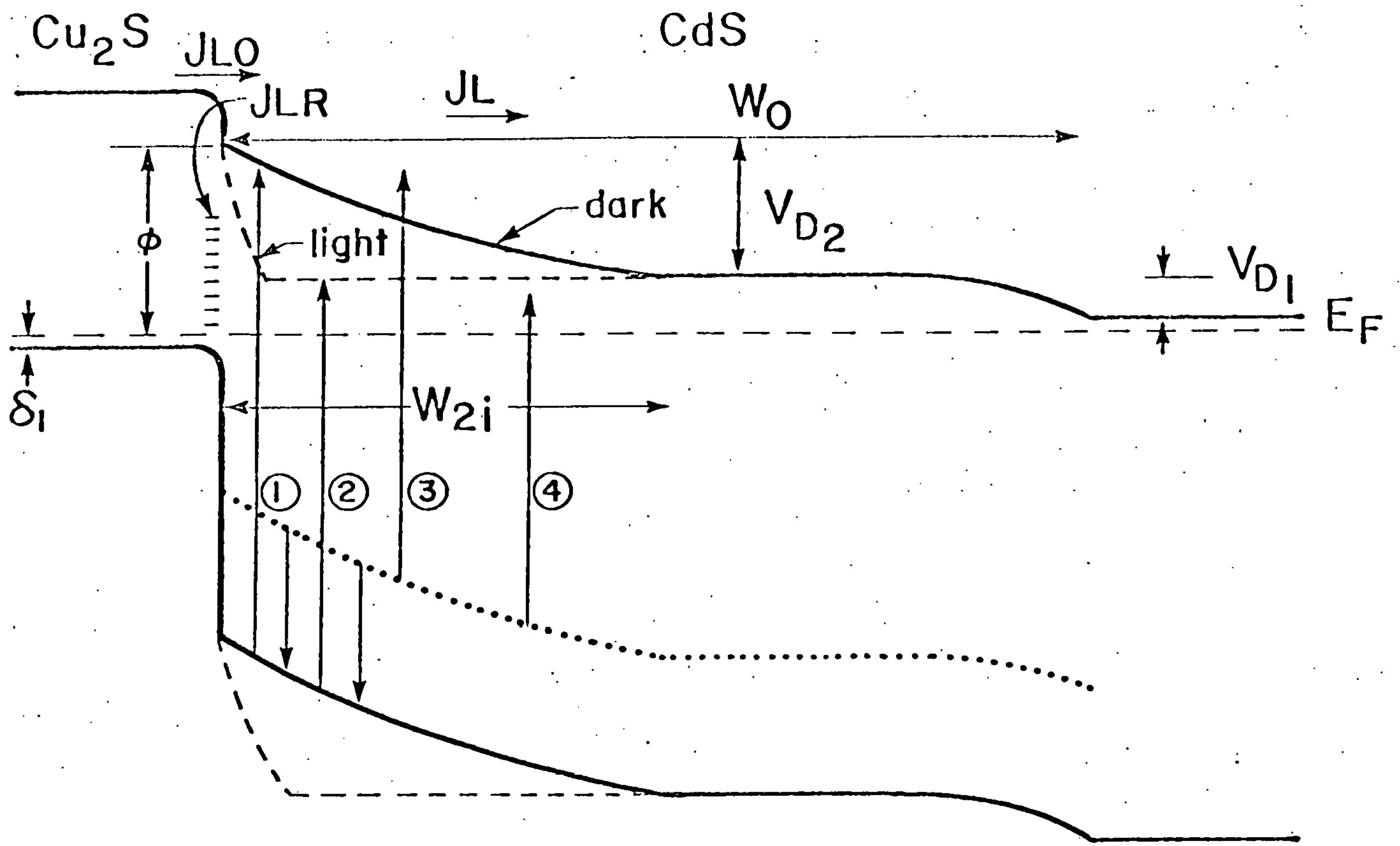

Fig. 2

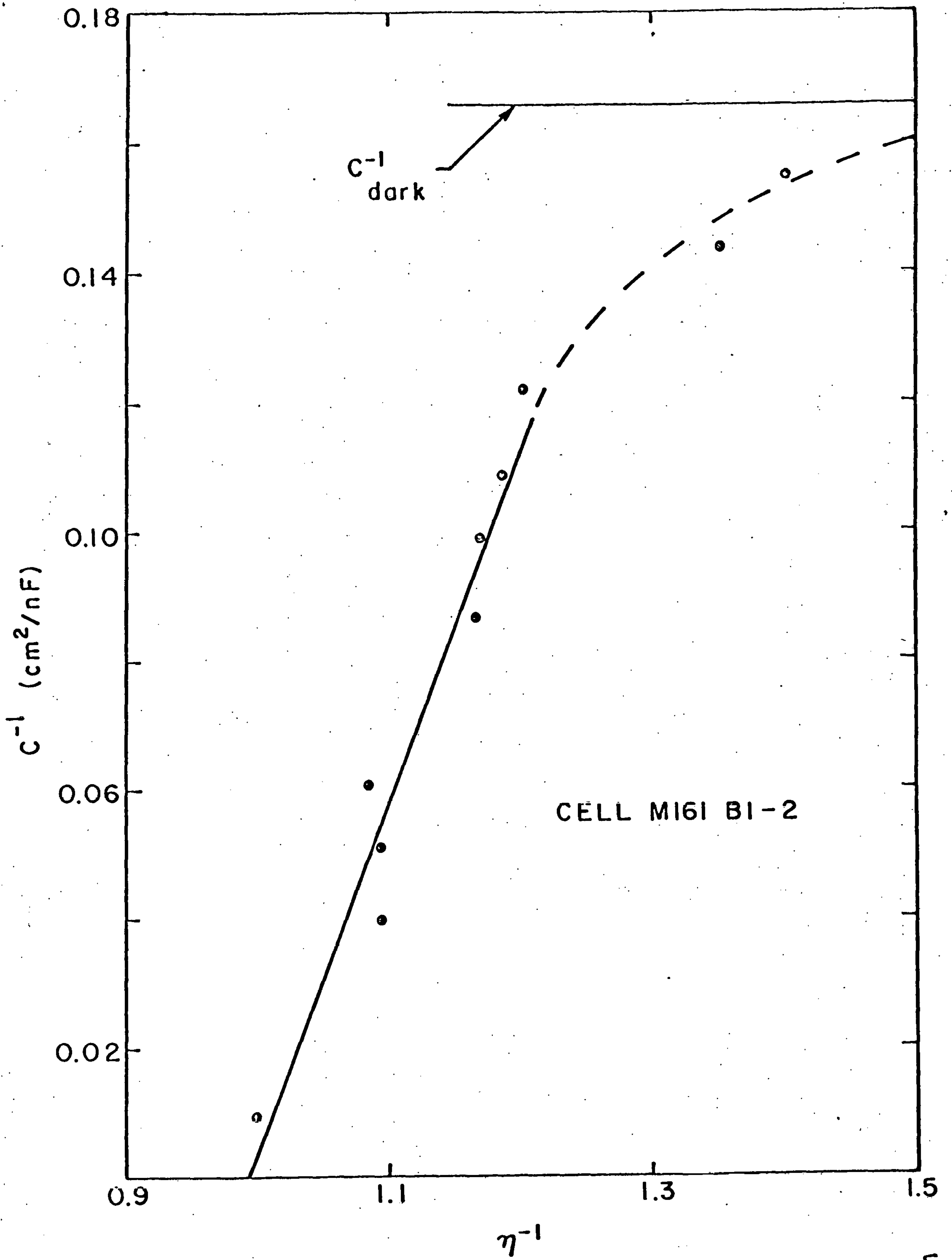

Fig. 3

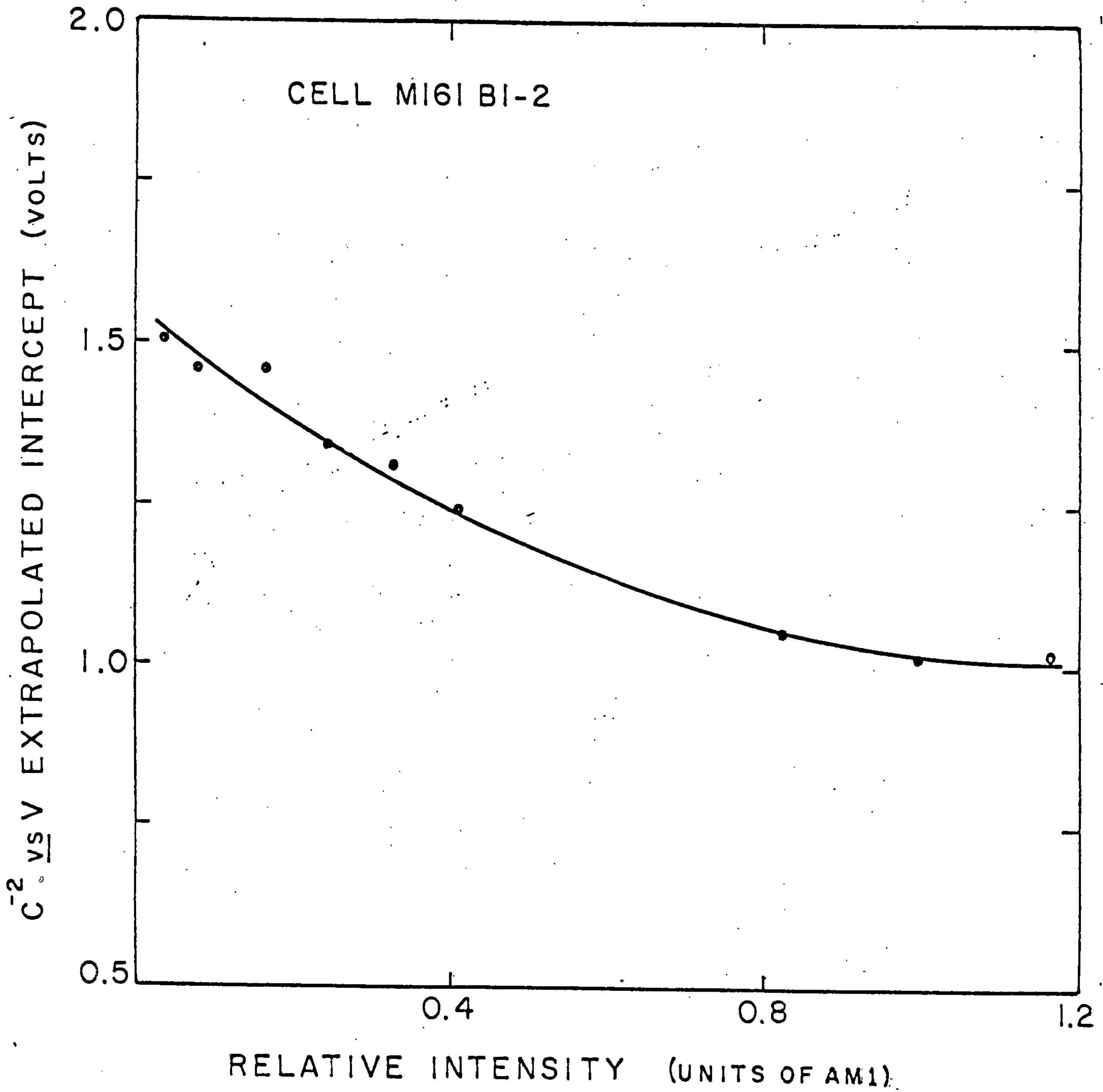

Fig. 4

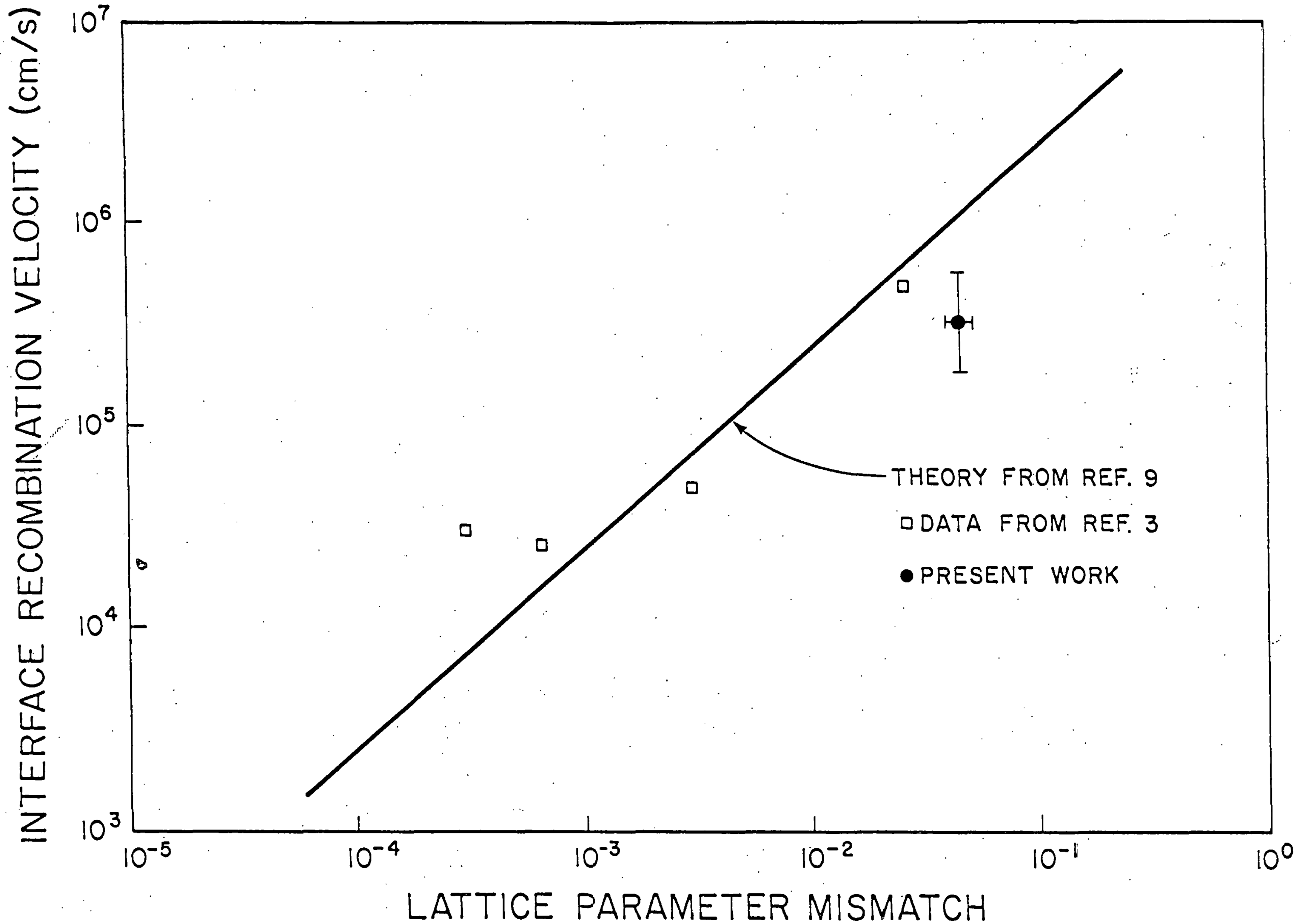

INTERFACE RECOMBINATION VELOCITY (cm/s)
10^7
10^6
10^5
10^4
10^3
10^{-5}
10^{-4}
10^{-3}
10^{-2}
10^{-1}
10^0
LATTICE PARAMETER MISMATCH
THEORY FROM REF. 9
DATA FROM REF. 3
PRESENT WORK